frontiers | Frontiers in Earth Science

TYPE Original Research
PUBLISHED 28 December 2023
DOI 10.3389/feart.2023.1269159

OPEN ACCESS

EDITED BY
Xiaoping Zhou,
Chongqing University, China

REVIEWED BY
Nan Xiao,
Changsha University of Science and Technology, China
Jian-Zhi Zhang,
Fuzhou University, China

*CORRESPONDENCE
Hongyan Qu,
hongyan.qu@cup.edu.cn

RECEIVED 29 July 2023
ACCEPTED 16 October 2023
PUBLISHED 28 December 2023

CITATION
Dong J, Qu H, Zhang J, Han F, Zhou F, Shi P, Shi J and Yu T (2023), Numerical simulation of hydraulic fracture propagation under energy supplement conditions.
Front. Earth Sci. 11:1269159.
doi: 10.3389/feart.2023.1269159

Numerical simulation of hydraulic fracture propagation under energy supplement conditions

Jingfeng Dong[1], Hongyan Qu[2,3,4]*, Jingchun Zhang[1], Feipeng Han[1], Fujian Zhou[2,3,4], Peize Shi[2,3], Jilong Shi[2,3] and Tianxi Yu[1]

[1]Engineering Technology Research Institute, PetroChina Xinjiang Oilfield Company, Karamay, Xinjiang, China, [2]National Key Laboratory of Petroleum Resources and Engineering, China University of Petroleum, Beijing, China, [3]Unconventional Petroleum Research Institute, China University of Petroleum, Beijing, China, [4]College of Artificial Intelligence, China University of Petroleum, Beijing, China

After the long-term production, due to the influence of low-pressure and low-stress fields in the near-well area, the reversion and propagation of new fractures after temporary plugging is short. It is difficult for the new fracture to extend to the remaining oil enrichment areas on both sides of the primary fractures, resulting in a low increase in the bandwidth of the fracture group after repeated fracturing, which affects the reservoir utilization. In the early stage of repeated fracturing, a large amount of pre-fracturing fluid is injected to supplement the energy of the fractures and rapidly increase the pore pressure in the local range, weakening rock strength and change the pore structure. In addition, the combination of energy replenishment and reservoir stimulation, coupled reconstruction of the seepage field and stress field, promotes the effective propagation of new fractures. However, in the process of increasing formation energy, the propagation law of hydraulic fractures and natural fractures is not clear. In this paper, the model of tight sandstone reservoir in the HQ block of Ordos Basin was established with the finite element software ABAQUS, based on the effective stress principle and the theoretical method of fluid-solid coupling numerical simulation. The propagation of a single hydraulic fracture and the interaction between hydraulic fracture and natural fracture under the condition of energy increase was investigated to better guide the field operation. The results show that for every 1 MPa pressure increase in a single hydraulic fracture, the fracture length increases by 0.62 m and the maximum fracture width decreases by 0.09 mm. When the formation energy increases by 6 MPa, the time for the hydraulic fracture to reach the intersection point with the natural fracture is shortened by 10 %, and the length of the natural fracture is 2.16 times compared with the case of 3 MPa energy increase.

KEYWORDS

energized fracturing, hydraulic fractures, numerical simulation, fluid-solid coupling, ABAQUS

1 Introduction

Unconventional tight reservoirs have poor physical properties and strong heterogeneity (Wang et al., 2017; Chai et al., 2023), and water channeling is common in conventional fracturing, the effect of water injection to supplement energy is poor (Wang et al., 2019). Water injection huff and puff technology is an important energy supplement method in the development of tight oil reservoirs (Pu et al., 2023). During the soaking process, the oil in the

matrix can be effectively replaced by dialysis, and the oil well production can be improved (Wang et al., 2018; Cui et al., 2023). However, water injection huff and puff have slow dialysis rates and low sweep degrees (Li and Fan, 2021), so it is necessary to find better methods to stimulate tight reservoirs.

The energized re-fracturing technology can increase the complexity of the reservoir fracture network and fully stimulate the reservoir while supplementing the formation energy (Fang et al., 2023). In the design of energized re-fracturing, optimizing the fracture parameters, fluid volume, and fracturing fluid system can effectively improve the production of oil wells (Zang and Chen, 2015). Because of the poor production effect of primary fracturing in tight reservoirs, the optimization of energized re-fracturing can effectively improve the recovery of reservoirs (Ren et al., 2020). The field pilot test of the network-enhanced re-fracturing technology for horizontal wells shows that the development effect of the block has been greatly improved (Fan et al., 2022). Energized re-fracturing can improve oilfield production and has a good effect on oil and gas production. It is necessary to clarify its internal mechanism to guide on-site stimulation operations.

With the increase of oil well development years, the formation energy is depleted, and a certain amount of energy storage medium is injected into the formation, which can increase the formation energy through the dialysis and diffusion in the formation (Wang, 2020; Da et al., 2021). Laboratory experiments and field experiments show that water injection can effectively supplement formation energy, enhance reservoir dialysis and drainage, and increase oil well production (Li, 2015a; Wu et al., 2017; Gao et al., 2018). The energy storage medium can weaken the strength of the formation rock and change the pore structure (Li, 2015b; Nowrouzi et al., 2020). The re-fracturing after energy storage can further increase the fracturing volume and fracture complexity (Huang et al., 2020; Wang et al., 2022). It is of great significance to study the influence of hydraulic fractures after energy storage and the interaction between hydraulic fractures and natural fractures on the stimulation of tight reservoirs. The numerical simulation method shows that the energy increase can increase the pore pressure of the formation, making the rock more likely to be destroyed along the weak surface, which is conducive to crack propagation (Guo et al., 2021). There are few studies on the effect of energy supplements before fracturing on reducing rock strength and the extension of new fractures, and the law of formation energy propagation during the period of shut-in after fracturing.

Due to the complexity of the environment in which the rock is located in the formation, appropriate numerical simulation models need to be used to characterize the fracture propagation. Chen et al. established a fully coupled cohesive finite element model, coupled fluid flow and elastic deformation, and quantitatively studied the interaction between hydraulic fractures and pre-existing natural fractures under various parameters (Chen et al., 2017). Li et al. established a three-dimensional model of stress-seepage-damage coupling in the cohesive zone. The interaction between hydraulic fractures and natural fractures can be simulated and analyzed with finite element method (Li et al., 2020).

Therefore, through theoretical analysis, this paper clarifies the necessity of collaborative solutions of the seepage field and stress field in the process of fracturing fluid-solid coupling. Based on the ABAQUS mechanical numerical simulation platform, a two-dimensional plane strain model is established with XFEM and the Cohesive bonding element to quantify the influence of different formation pressures on a single fracture propagation and the interaction between hydraulic fractures and natural fractures.

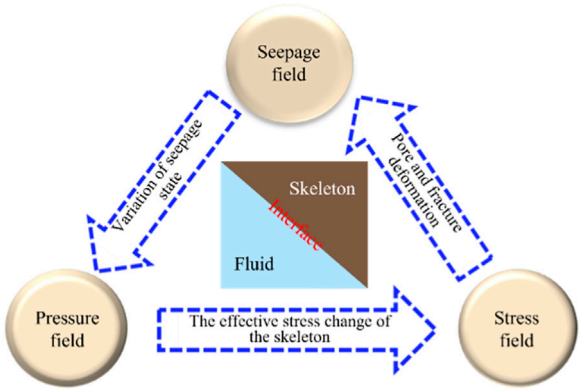

FIGURE 1
Fluid-solid interaction.

2 Methods and Theories

2.1 Numerical method

According to the principle of effective stress, the compressive stress of overburden is shared by the rock skeleton and fluid in pores. During the fracturing process, high-energy fluid entering the pores of porous media redistributes the pressure in the pores and changes the pressure field. The variation of pressure in the pore changes the effective stress of the rock skeleton, thus changing the stress field of the rock. The variation of effective stress results in changes in reservoir parameters such as porosity and permeability, and affects the seepage field (Peng et al., 2021). Therefore, the fracturing process is accompanied by the coupling of porous flow and stress fields between fluid and rock skeleton (Figure 1).

Porous flow and deformation occur at the same time, and both should be taken into consideration in the study of coupling problems. If the cross-iterative coupling method is adopted to calculate the porous flow field with a given displacement and stress field with given pressure, the error is larger than the actual situation (Tan et al., 2021). To study the influence of energy supplement on hydraulic fracture propagation, the mechanical simulator ABAQUS was used to investigate both displacement and pressure. The equations of stress balance and fluid continuity were solved cooperatively.

2.2 Governing equation

2.2.1 Effective stress principle

Suppose there is a medium composed of solid particles and fully saturated pores of wettable fluid, and the linear momentum balance conservation equation is as follows (Rueda et al., 2020):

$$\nabla \cdot \sigma + \rho g = 0 \tag{1}$$

where σ is the stress tensor, N/m^2, ρ is the density of porous media, kg/m^3; g is the gravity vector, m/s^2.

The total stress in porous media consists fluid pressure of pores and the 'effective stress' of the medium skeleton:

$$\sigma = \bar{\sigma} - \alpha P \tag{2}$$

where $\bar{\sigma}$ is the effective stress tensor (compression is negative), N/m^2; α is the Biot coefficient, dimensionless; P is pore pressure, Pa. Among them:

$$\alpha = 1 - \frac{K}{K_s} \tag{3}$$

where K is the deformation modulus of the porous medium, Pa; K_s is the deformation modulus of the medium without pore volume, Pa. For incompressible solid particles, $K_s \to \infty$ and $\alpha = 1$.

2.2.2 Stress balance equation

The stress equilibrium of the material solid phase can be expressed by the virtual work principle (Wang et al., 2015) under the current configuration of the volume under consideration at time t:

$$\int_V (\bar{\sigma} - \rho_w I)\delta\varepsilon dV = \int_S t \cdot \delta v dS + \int_V f \cdot \delta v dV \tag{4}$$

where t is the surface traction vector per unit area, N/m^2; ρ_w is the fluid density, kg/m^3; I is the identity matrix, dimensionless; $\delta\varepsilon$ is the virtual strain velocity matrix, s^{-1}; f is the physical force vector per unit volume, N/m^3; δv is the virtual velocity matrix, m/s.

2.2.3 Fluid flow equation

The continuity equation of saturated fluid in porous media is (Zhang et al., 2011):

$$\frac{1}{J}\frac{\partial}{\partial t}(J\rho_w) + \frac{\partial}{\partial x}(\rho_w n_w v_w) = 0 \tag{5}$$

where J is the volume change rate of the porous medium, dimensionless; X is the space vector m; n_w is the porosity, dimensionless; v_w is the velocity of flow, m/s.

Instead of porosity, the ratio of pore volume to skeleton volume is used in ABAQUS:

$$n_w = \frac{V_v}{V_g} \tag{6}$$

where V_v is the pore volume, m^3; V_g is the skeleton volume, m^3.

It is assumed that the flow velocity of the fluid is low. According to Darcy's law, the flow velocity of the fluid in the porous medium is:

$$v_w = -\frac{1}{\rho_w g n_w} k\left(\frac{\partial \rho_w}{\partial x} - \rho_w g\right) \tag{7}$$

where k is the matrix permeability coefficient, m/s.

2.3 Cohesive traction-separation law

In ABAQUS modeling, the Cohesive zone model based on damage mechanics is established by Cohesive elements on possible fracture propagation paths. In this model, the Traction-separation law controls the rock damage and hydraulic fracture propagation process (Gao et al., 2019; Luo et al., 2023). There is a double linear relationship between the traction force and the separation between the two fracture planes at the fracture tip. When the traction force reaches the maximum value, the traction force increases linearly with the increase of the distance between the two fractured surfaces. While as the separation increases, the traction decreases linearly, and when the traction decreases to 0, a new fracture unit will be generated (Figure 2).

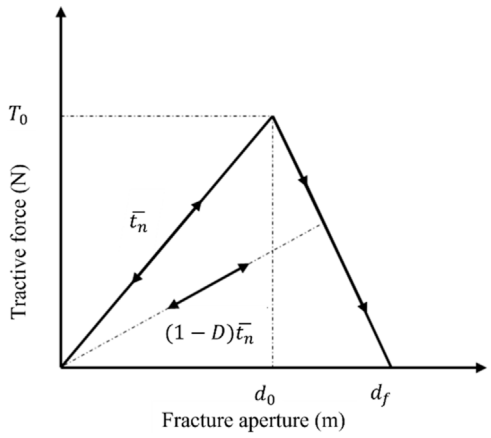

FIGURE 2
Traction-separation law.

2.3.1 Constitutive equation

It is assumed that linear elastic deformation occurs initially after rock damage, and its elastic constitutive equation (Zou et al., 2021) is:

$$\begin{Bmatrix} t_n \\ t_s \\ t_t \end{Bmatrix} = \frac{E(1-\nu)}{(1+\nu)(1-2\nu)} \begin{bmatrix} 1 & 0 & 0 \\ 0 & \frac{1-2\nu}{2(1-\nu)} & 0 \\ 0 & 0 & \frac{1-2\nu}{2(1-\nu)} \end{bmatrix} \begin{Bmatrix} \varepsilon_n \\ \varepsilon_s \\ \varepsilon_t \end{Bmatrix} \tag{8}$$

where t_n is the normal component of the traction stress vector, N/m^2; t_s and t_t are tangential components of the traction stress vector, N/m^2; E is the elastic modulus, GPa; ν is Poisson's ratio, dimensionless; ε is strain, dimensionless.

2.3.2 Fracture initiation criterion

To ensure better convergence and stability in the hydraulic fracturing calculation, the maximum principal stress criterion is adopted to characterize the initial damage of fracture initiation (Haddad and Sepehrnoori, 2016):

$$f = \left\{\frac{\sigma_{\max}}{\sigma^0_{\max}}\right\} \tag{9}$$

where f is the maximum principal stress coefficient, dimensionless; $\sigma_{\max}$、$\sigma^0_{\max}$ are the maximum principal stress and the maximum allowable principal stress respectively, Pa. When f reaches the critical value 1, the fracture starts in the direction perpendicular to the maximum tensile stress.

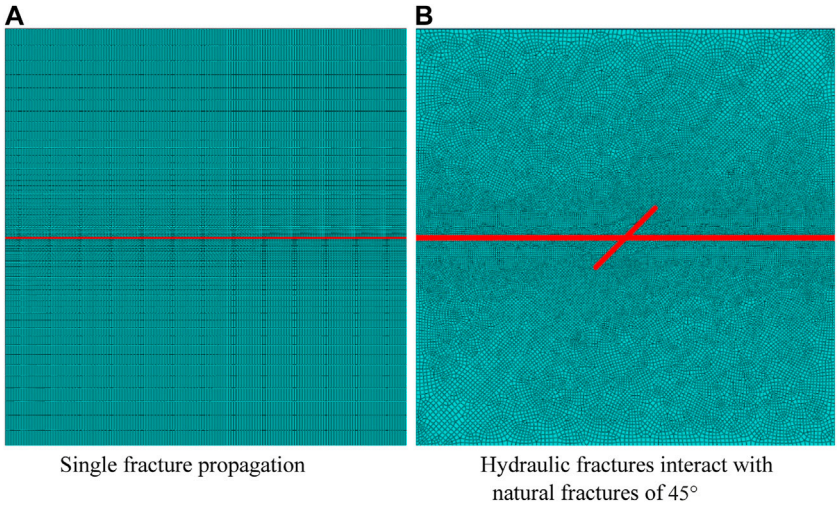

FIGURE 3
Finite element model. **(A)** Single fracture propagation, **(B)** Hydraulic fractures interact with natural fracture of 45°.

2.3.3 Damage evolution criterion

The damage evolution law characterizes the degradation rate of the material stiffness reaching the fracture initiation criterion. The displacement damage evolution criterion is adopted in this paper:

$$t_n = \begin{cases} (1-D)\overline{t_n}, & \overline{t_n} \geq 0 \\ \overline{t_n}, & \overline{t_n} < 0 \end{cases} \quad (10)$$

$$t_s = (1-D)\overline{t_s} \quad (11)$$

$$t_t = (1-D)\overline{t_t} \quad (12)$$

where D is the damage factor of the material, dimensionless, which includes the combined effect of all mechanisms, the initial value is 0, and D evolves from 0 to 1 after the damage starts and after further loading. $\overline{t_n}$、 $\overline{t_s}$、 $\overline{t_t}$ are the stress components predicted by elastic traction separation behavior of current strain without damage, N/m^2.

$$D = \frac{\delta_m^f\left(\delta_m^{\max} - \delta_m^0\right)}{\delta_m^{\max}\left(\delta_m^f - \delta_m^0\right)} \quad (13)$$

where δ_m^0 is the effective displacement at the beginning of damage, m; $\delta_m^{\max}$ is the maximum effective displacement obtained in the loading process, m.

3 Model establishment

Based on the ABAQUS finite element simulation platform, two finite element numerical models of hydraulic fracturing are established based on the Cohesive element. The first model simulates the effect of increasing formation energy on the propagation of a single fracture. The second model simulates the effect of increased formation energy on the interaction pattern between hydraulic fractures and natural fractures at an angle of 45°. A two-dimensional plane strain model is used to simulate the fracture propagation of hydraulic fracturing. The CPE4P quadrilateral pore pressure element was used and the COH2D4P element (bonding element) was embedded to the possible fracture propagation path. The grid division of the above two models is shown in Figure 3. The grid near the hydraulic fracture is finely meshed to ensure the accuracy and convergence of the calculation results.

TABLE 1 Basic modeling parameters.

Parameter	Value	Unit
Average porosity ($\bar{\varnothing}$)	12	(%)
Average permeability ($\bar{k}$)	0.4	mD
Rock elastic modulus (E)	22	GPa
Poisson's ratio of rock (v)	0.22	-
Tension strength of rock (T_r)	6	MPa
Tensile strength of natural fracture (T_f)	3	MPa
Injection rates (q)	2	m^3/min
Maximum horizontal principal stress (σ_{max})	34	MPa
Minimum horizontal principal stress (σ_{min})	30	MPa

The finite element model was established based on the tight sandstone reservoir parameters of the HQ block in the Ordos Basin. The model size was 60 × 60 m. The basic parameters of the model are shown in Table 1.

4 Results and discussions

4.1 Influence of pressure increase on propagation of a single hydraulic fracture

The Cohesive unit was used to simulate the propagation of a single hydraulic fracture under the condition of increasing different

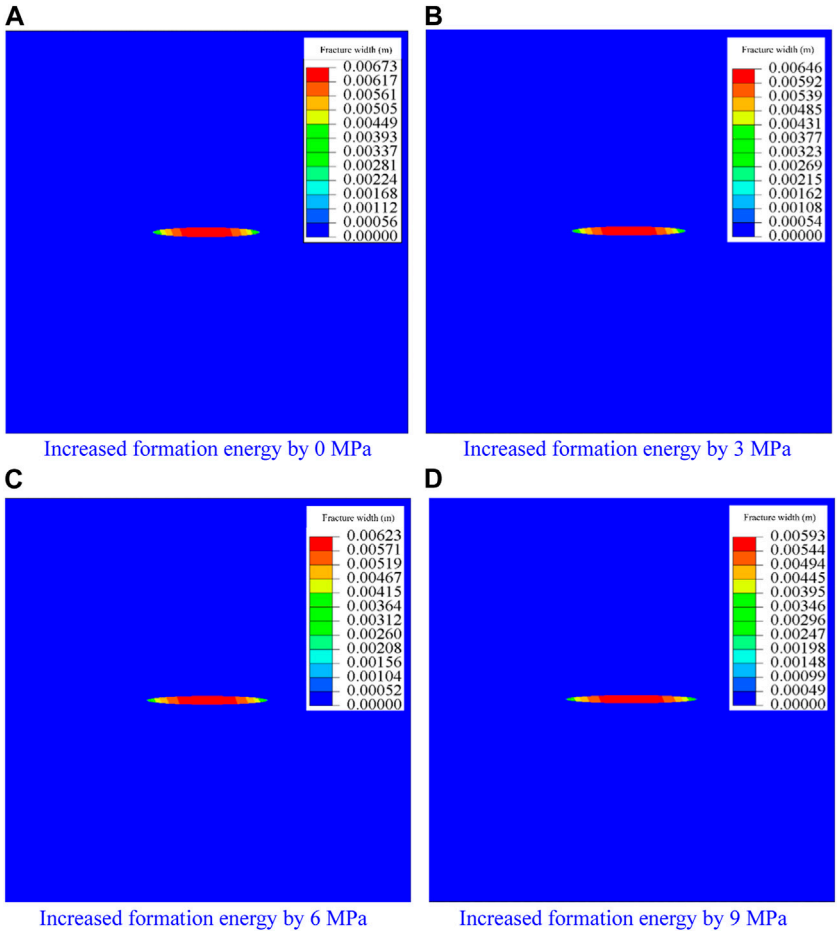

FIGURE 4
Single crack propagation morphology under increasing formation energy conditions. **(A)** Increased formation energy by 0 MPa, **(B)** Increased formation energy by 3 MPa, **(C)** Increased formation energy by 6 MPa, **(D)** Increased formation energy by 9 MPa.

formation pressures (Figure 4). The formation pressure was increased by 0, 3, 6, and 9 MPa to ensure the same injection rate and injection duration. As can be seen from the cloud map results, with the increase of formation energy, the extension distance of hydraulic fracture propagation becomes longer, but the total injected liquid remains unchanged, so the fracture width decreases to some extent.

To more intuitively reflect the different forms of hydraulic fractures, the displacement of the grid element at the fracture position under different energy-increasing conditions is extracted, and the relationship between fracture length and fracture width is demonstrated (Figure 5), along half of the fracture propagation path. After increasing the formation energy, the effective stress on the rock skeleton is substantially reduces, promotes the fracture to continue to extend forward (Zhou et al., 2022), increases the possibility of hydraulic fracture extending to the remaining oil enrichment area, and then improves the reservoir utilization.

To quantitatively evaluate the influence of energy increase on hydraulic fracture propagation, the relationship between different formation energy and fracture parameters is illustrated (Figure 6). When the formation energy does not increase, the hydraulic fracture length is 26.4 m and the maximum fracture width is 6.732 mm. The formation energy increases by 3, 6, and 9 MPa respectively, the hydraulic fracture length increases to 28, 29.6, and 32 m, with an increase of 6.06%, 5.71%, and 8.11% respectively, and the maximum fracture width decreases to 6.46, 6.23 mm and 5.93mm, with a decrease of 4.04%, 3.56% and 4.82% respectively. For every 1 MPa increase in formation energy, the hydraulic fracture length increases by 0.62 m, and the maximum fracture width decreases by 0.09 mm.

From the above results, it can be seen that when other conditions remain unchanged, the fluid is injected before fracturing to quickly supplement the depleted formation energy in the near-wellbore area. The well is then shut down for about 2 h, so that the pressure field and stress field are quickly balanced in the local range, and a local high-pressure field is formed, which is conducive to the extension of new fractures in the subsequent stimulation stage. The longer the diffusion time, the larger the energy supplement range, but the smaller the energy supplement increment. Therefore, the diffusion time should proper, and the pressure should be diffused to the residual oil boundary so that the hydraulic fracture can be effectively extended to the high-pressure unexploited area.

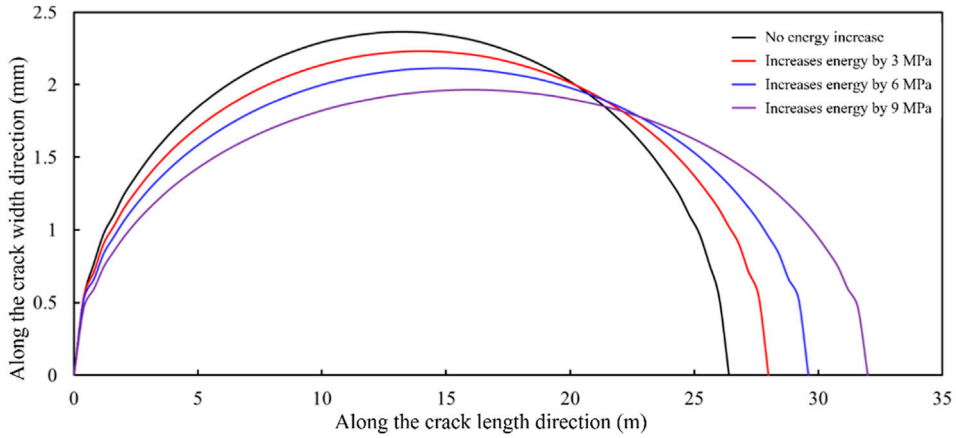

FIGURE 5
Crack propagation patterns under different energy-increasing conditions.

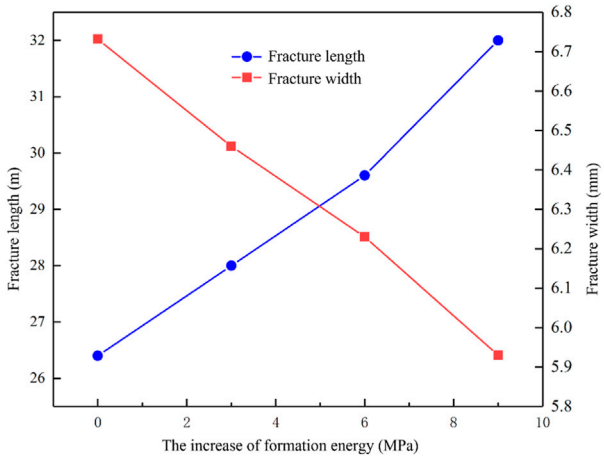

FIGURE 6
Crack parameters under different energization effects.

4.2 Effect of energy increase on the interaction between hydraulic fractures and natural fractures

A natural fracture with a dip angle of 45° and a total length of 10 m is preset in the center of the model. The injection point is at the center of the left boundary of the model to simulate the effect of increasing different formation energy on activating natural fractures, which can be directly reflected in the fracture width cloud map (Figure 7). Under the premise of constant injection rate and time, increasing formation energy is conducive to opening natural fractures with the same approximation angle. In addition, the crack width shows a decreasing trend, which is consistent with the understanding obtained in the previous section.

To quantitatively characterize the effect of energy increase on the activation of natural fractures, the length and time of the opened natural fracture branches were extracted and the relationship chart was demonstrated (Figure 8). Under the condition of initial formation pressure, the length of hydraulic fracture is only 18.48 m at the end of fracturing, and the distance from the interaction position with a natural fracture is 6.52 m. When the formation pressure is increased by 3 MPa, the hydraulic fracture has reached the intersection point when the injection time is 206.4 s, but the upper half of the natural fracture is not fully opened, and the activation part is only 2.06 m. When the formation energy increases by 6 MPa, at 188.8 s, the hydraulic fracture reaches the intersection position, and the upper half of the natural fracture is fully activated after the fracturing, which is 4.46 m. When the formation energy is increased by 9 MPa, the upper half of the natural fracture is also completely opened, which is 5.00 m, but it reaches the intersection point earlier, at 176 s. Due to the opening of natural fractures, the surrounding reservoir rocks are squeezed to form a local high-stress field. Since then, the width of natural fractures has decreased, and hydraulic fractures tend to continue to extend along the original path (Figure 7D). From the above results, it can be seen that by increasing the formation energy, natural fractures are inclined to shear failure, which can become a channel for oil and gas flow, help more oil and gas to be mined, and improve the productivity of oil wells. In this case, the angle between the lower half branch of the natural fracture and the hydraulic fracture is obtuse, and it has not been opened, which is the same conclusion as that studied by Zhou et al. (2020); Bi and Zhou (2015), demonstrating that the effect of increasing the opening of the natural fracture is limited. In repeated fracturing, the net pressure in the fracture should be combined with temporary plugging to open the natural fracture to a greater extent, activate the original formation energy in a larger range to increase production, further improve the complexity of the fracture, and accelerate the oil drainage between the matrix and the fracture.

5 Conclusion

(1) The injection of high-pressure fluid causes a two-field coupling of seepage and stress in the initial fracture range. Fluid seepage and rock deformation occur at the same time. The coupling problem needs to be considered at the same time. The stress

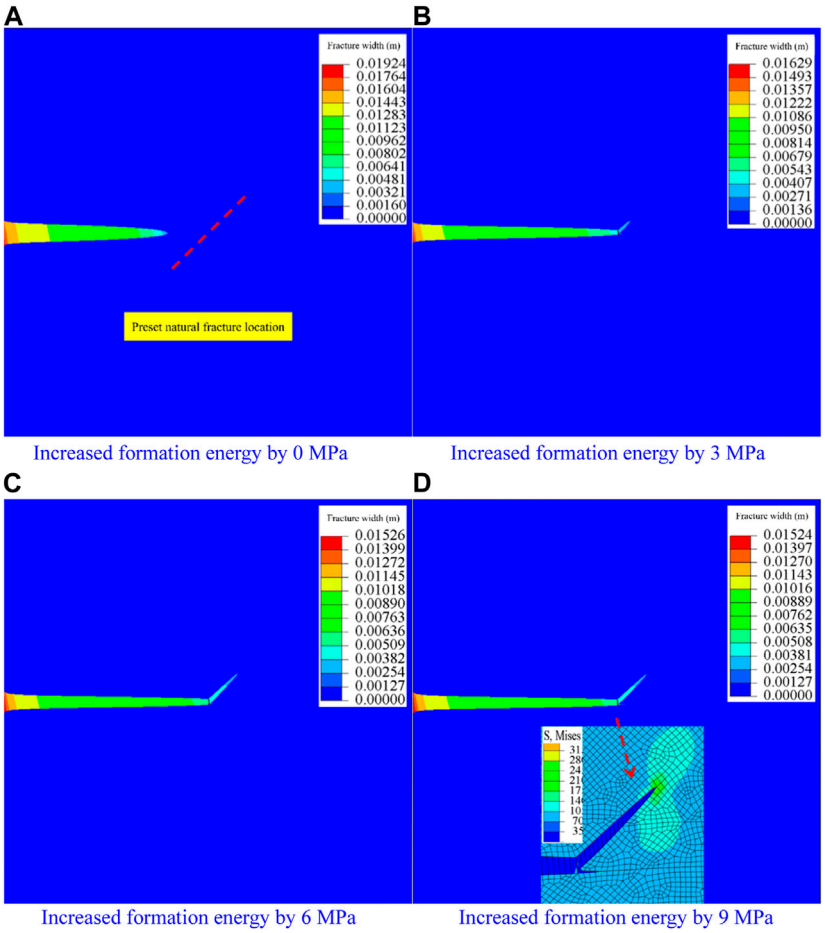

FIGURE 7
Open natural cracks under different conditions of increasing formation energy. **(A)** Increased formation energy by 0 MPa, **(B)** Increased formation energy by 3 MPa, **(C)** Increased formation energy by 6 MPa, **(D)** Increased formation energy by 9 MPa.

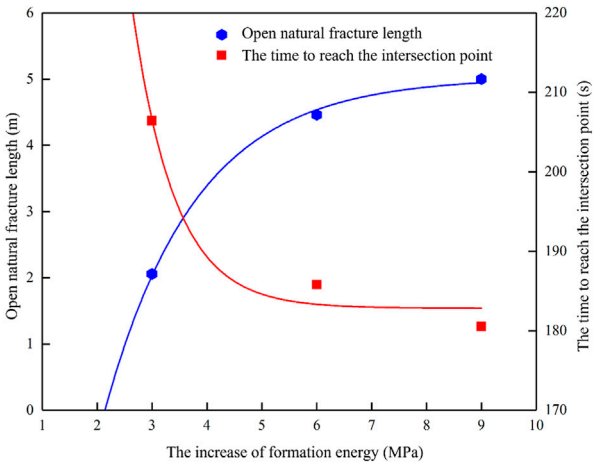

FIGURE 8
Crack parameters under different energization effects.

balance equation and fluid continuity equation are solved cooperatively.

(2) After increasing formation pressure, longer hydraulic fractures can be formed under the same injection rate and injection volume, even if the fracture width is reduced. For every 1 MPa increase in formation energy, the hydraulic fracture length increases by 0.62 m, and the maximum fracture width decreases by 0.09 mm. It promotes the effective extension of hydraulic fractures from depleted low-pressure and low-stress areas to high-pressure and high-stress areas, increases the contact area between fractures and matrix, and provides more seepage channels for oil and gas exploitation.

(3) Under the condition of formation energy deficit, it is difficult for hydraulic fractures to open natural fractures. However, when the formation energy is supplied in advance, the intersection time between the hydraulic fracture and the natural fracture is shortened, and the larger natural fracture is opened. The simulation results show that when the

formation energy is increased by 6 MPa, the time to reach the intersection point is shortened by 10%, and the energy is increased by 2.16 times.

Data availability statement

The original contributions presented in the study are included in the article/Supplementary material, further inquiries can be directed to the corresponding author.

Author contributions

JD: Conceptualization, Supervision, Funding acquisition, Writing–original draft, Writing–review & editing. HQ: Conceptualization, Writing–original draft, Writing–review & editing, Investigation, Resources, Supervision, Funding acquisition, Validation. JZ: Funding acquisition, Writing–original draft, Writing–review & editing. FH: Data curation, Writing–original draft, Writing–review & editing. FZ: Writing–original draft, Writing–review & editing, Methodology, Project administration. PS: Data curation, Writing–original draft, Writing–review & editing, Software, Formal Analysis, Methodology, Visualization. JS: Data curation, Writing–original draft, Writing–review & editing, Visualization. TY: Data curation, Writing–original draft, Writing–review & editing.

Funding

The author(s) declare financial support was received for the research, authorship, and/or publication of this article. This work is supported by the National Natural Science Foundation of China (Grant Nos 52174044 and 52004302), Science Foundation of China University of Petroleum, Beijing (Nos ZX20200134 and 2462021YXZZ012).

Conflict of interest

JD, JZ, FH, and TY was employed by the company PetroChina Xinjiang Oilfield Company.

The remaining authors declare that the research was conducted in the absence of any commercial or financial relationships that could be construed as a potential conflict of interest.

The authors declare that this study received funding from Major Project of PetroChina (Grant No. 2022KT1704) and the Strategic Cooperation Technology Projects of CNPC and CUPB (ZLZX 2020-01-07). The funders had the following involvement in the study: supervision, funding acquisition, writing–original draft, writing–review & editing.

Publisher's note

References

Bi, J., and Zhou, X. P. (2017). A novel numerical algorithm for simulation of initiation, propagation and coalescence of flaws subject to internal fluid pressure and vertical stress in the framework of general particle dynamics. *Rock Mech. Rock Eng.* 50, 1833–1849. doi:10.1007/s00603-017-1204-4

Chai, X., Tian, L., Yan, MENG, et al. (2023). Study on characteristics and classification of micro-pore structure in tight reservoirs for Ordos Basin. *Nat. Gas. Geosci.* 34 (1), 51–59.

Chen, Z., Jeffrey, R. G., Zhang, Xi, and Kear, J. (2017). Finite-element simulation of a hydraulic fracture interacting with a natural fracture. *SPE J.* 22, 219–234. doi:10.2118/176970-pa

Cui, P., Hou, B., and Meng, X. (2023). Micro-scale oil and water migration characteristics of water-injection huff and puff in ultra-low permeability reservoirs. *Xinjiang Oil Gas.* 19 (1), 8–15. doi:10.12388/j.issn.1673-2677.2023.01.002

Da, Y., Xue, X., and Liu, M. (2021). Energy enhancement mechanism of energy storage refracturing in ultra-low permeability oil fields. *Sci. Technol. Eng.* 21 (33), 14139–14146. doi:10.3969/j.issn.1671-1815.2021.33.015

Fan, L., Liu, R., and Wang, H. (2022). Refracturing technology for tight oil horizontal well network energy enhancement. *Chem. Eng. Equip.* (08), 72–74.

Fang, L., Wang, J., and Yuan, Y. (2023). Application practice of energy storage volume fracturing in tight sandstone reservoir of fault block A. *Petrochem. Appl.* 42 (05), 15–19. doi:10.3969/j.issn.1673-5285.2023.05.004

Gao, Qi, Han, S., Cheng, Y., Yan, C., Sun, Y., and Han, Z. (2019). Effects of non-uniform pore pressure field on hydraulic fracture propagation behaviors. *Eng. Fract. Mech.* 221, 106682. doi:10.1016/j.engfracmech.2019.106682

Gao, T., Zhao, X., and Dang, H. (2018). The mechanism and application of water injection huff and puff in tight reservoirs of Yanchang oilfield. *Spec. Reserv.* 25 (04), 134137. doi:10.3969/j.issn.1006-6535.2018.04.027

Guo, J., Zhou, F., Hu, X., et al. (2021). Mechanical mechanism of energy-increasing fracturing for tight oil horizontal wells in Santanghu Basin. *Fault block oil gas field* 28 (01), 57–62.

Haddad, M., and Sepehrnoori, K. (2016). XFEM-Based CZM for the simulation of 3D multiple-cluster hydraulic fracturing in quasi-brittle shale formations. *Rock Mech. rock Eng.* 49 (12), 4731–4748. doi:10.1007/s00603-016-1057-2

Han, Y. (2015). Numerical modeling of non-planar hydraulic fracture propagation in brittle and ductile rocks using XFEM with cohesive zone method. *J. Petroleum Sci. Eng.* 135, 127–140. doi:10.1016/j.petrol.2015.08.010

Huang, T., Su, L., and Da, Y. (2020). Mechanism study and field test of energy storage fracturing for horizontal wells in ultra-low permeability reservoirs. *Oil Drill. Technol.* 48 (01), 80–84. doi:10.11911/syztjs.2020024

Li, B., and Fan, L. (2021). Research progress of tight oil reservoir mining technology. *Petrochem. Appl.* 40 (11), 1–6. doi:10.3969/j.issn.1673-5285.2021.11.001

Li, M., Hu, X., and Zhou, F. (2020). "Three-dimensional numerical simulation of interaction of hydraulic fracture and natural fracture using the cohesive zone finite element method," in *Proceedings of the SPE/AAPG/SEG Latin America unconventional resources technology conference* Virtual. doi:10.15530/urtec-2020-1380

Li, X. (2015a). Exploration of tight oil water injection huff and puff oil recovery technology in Tuha Oilfield. *Special oil gas reservoirs* 22 (04), 144146+158.

Li, X. (2015b). Exploration of tight oil water injection huff and puff oil recovery technology in Tuha Oilfield. *Special oil gas reservoirs* 22 (4), 144146+158.

Luo, Y., Kong, H., Xu, K., et al. (2023). Numerical simulation for vertical propagation pattern of hydraulic fractures in sand-shale in-terbedded reservoirs. *Xinjiang Oil Gas* 19 (1), 49–56.

Nowrouzi, I., Abbas, K. M., and Amir, H. (2020). The mutual effects of injected fluid and rock during imbibition in the process of low and high salinity carbonated water injection into carbonate oil reservoirs. *J. Mol. Liq.* 305 (112432), 112432. doi:10.1016/j.molliq.2019.112432

Peng, N., Ma, T., and Chen, P. (2021). Fully coupled thermal-hydro-mechanical model of pore pressure propagation around borehole with dynamic mudcake growth. *J. Nat. Gas Sci. Eng.* 96, 104330. doi:10.1016/j.jngse.2021.104330

Pu, C., Kang, S., and Pu, J. (2023). Progress and development trend of water huff-n-puff technology for horizontal wells in tight oil reservoirs in China. *Acta Pet. Sin.* 44 (1), 188–206. doi:10.7623/syxb202301012

Ren, J., Wang, X., Zhang, X., et al. (2020). Simulation of re-fracturing and fracture parameter optimization of horizontal wells in Daqing tight oil reservoir. *Fault block oil gas field* 27 (05), 638–642.

Rueda, J., Mejia, C., Quevedo, R., and Roehl, D. (2020). Impacts of natural fractures on hydraulic fracturing treatment in all asymptotic propagation regimes. *Mech. Eng.* 371, 113296. doi:10.1016/j.cma.2020.113296

Tan, P., Jin, Y., and Pang, H. (2021). Hydraulic fracture vertical propagation behavior in transversely isotropic layered shale formation with transition zone using XFEM-based CZM method. *Eng. Fract. Mech.* 248, 107707. doi:10.1016/j.engfracmech.2021.107707

Wang, C., Zhu, W., and Cui, W. (2022). "Extending the Life Cycle of Old Wells: fracturing and replenishing formation energy at the same time," in *Proceedings of the paper presented at the offshore technology conference asia, virtual and kuala lumpur* Malaysia. doi:10.4043/31560-MS

Wang, W. (2020). Energy storage fracturing technology for old wells in low permeability oilfield. *Pet. Knowl.* (03), 58–59.

Wang, W., Peng, H., Li, G., et al. (2019). Waterflooding and optimum displacement pattern for ultra-low permeability reservoirs. *Oil Gas. Geol.* 40 (1), 182–189.

Wang, Z., Yang, S., and Wu, R. (2018). Influencing factors and mechanism of imbibition oil recovery in tight reservoirs. *Pet. Geol. Dev. Daqing* 37 (06), 158163. doi:10.19597/j.issn.1000-3754.201712016

Wang, J., Tian, J., and Wang, Z. (2017). "Optimization of water injection policy for horizontal wells in tight oil with low pressure," in *Proceedings of the SPE Russian petroleum technology conference* Moscow, Russia. doi:10.2118/187695-MS

Wang, T., Cheng, L., Xiang, Y., et al. (2023). Numerical simulation of fracture propagation pattern in the presence of gravel. *Xinjiang Oil Gas* 19 (1), 42–48.

Wu, Z., Zeng, Q., and Jin, Li (2017). A new way to effectively supplement formation energy development by water injection huff and puff in volume-modified reservoirs. *Oil Gas. Geol. recovery* 24 (5), 78–83+92. doi:10.13673/j.cnki.cn37-1359/te.2017.05.012

Yan, Y., Li, Ya, Guo, S., et al. (2021). Research and application of rock brittleness evaluation method based on compressive deformation characteristics. *Xinjiang Oil Gas.* 17 (04), 21–27. doi:10.3969/j.issn.1673-2677.2021.04.005

Zhang, G., Liu, H., Zhang, J., et al. (2011). Three-dimensional finite element numerical simulation of horizontal well hydraulic fracturing. *Eng. Mech.* 28 (2), 101–106.

Zhang, H., and Chen, J. (2015). Research on energy storage integral fracturing technology in low permeability oilfield-Taking the peripheral well area of Jilin oilfield as an example. *Unconv. oil Gas.* 2 (05), 55–60. doi:10.3969/j.issn.2095-8471.2015.05.010

Zhou, X., Du, E., and Wang, Y. (2022). Thermo-hydro-chemo-mechanical coupling peridynamic model of fractured rock mass and its application in geothermal extraction. *Comput. Geotech.* 148, 104837. doi:10.1016/j.compgeo.2022.104837

Zhou, X. P., Wang, Y. T., and Shou, Y. D. (2020). Hydromechanical bond-based peridynamic model for pressurized and fluid-driven fracturing processes in fissured porous rocks. *Int. J. Rock Mech. Min. Sci.* 132, 104383. doi:10.1016/j.ijrmms.2020.104383

Zou, J., Jiao, Y.-Y., Tan, F., Lv, J., and Zhang, Q. (2021). Complex hydraulic-fracture-network propagation in a naturally fractured reservoir. *Comput. Geotechnics* 135, 104165. doi:10.1016/j.compgeo.2021.104165